Stockholm University

Bachelor Thesis

Degree Project in Marine Geology 15 hp

Grain-size distribution profiles of deep sea carbonate sediments tested with a laser particle analyzer

Skander Chadli

Stockholm 2015

Department of Geological Sciences
Stockholm University
SE-106 91 Stockholm

Table of Contents

Grain size distribution profiles of deep sea carbonate sediments tested with a laser particle analyzer

Abstract

The thesis is focused on determining $CaCO_3$ particle size distributions in deep sea sediment samples to improve understanding of the types and relative proportions of planktonic contributors to bulk sediment $CaCO_3$, and thus the resulting water column palaeoceanographic signals obtainable from bulk $CaCO_3$ stable isotopes analysis. The results show that the laser particle analyzer is capable of generating particle distribution profiles to enable comparison between bulk sediment and acidified 'residual' components, and that comparison of the two allows estimates of the bulk $CaCO_3$ component. The thesis evaluates a set of limitations provided by the method using the laser particle analyzer.

Introduction

Different types of organisms contribute to the bulk carbonate in marine sediments. In open-ocean conditions coccoliths and planktonic foraminifera stand for the major contribution to the bulk carbonate, with minor influences of calcareous dinoflagellate cysts and benthic foraminifera. Attempts have been made to separate and quantify the different contributions of foraminifers and coccoliths for further investigations. Frenz, et al. 2005 successfully used grain size to study surface sediments in the south Atlantic to estimate the different carbonate products in different environments.

The purpose of this project was to determine $CaCO_3$ particle size distributions in deep sea sediment samples and in that way make an attempt in gaining more knowledge about what exact particles that are making up the bulk carbonate since different microfossils have different particle sizes. This information will be useful to the work of Daniele Reghellin (PhD-student, IGV), who is measuring bulk stable isotopes in bulk marine sediments. By knowing what particles that are making up the carbonate in a marine sediment, these could provide a ground testing for further studies about the kind of geochemical palaeoceanographic signals and thus oceanic conditions that the bulk isotopes are recording. For example, the small coccoliths would give a signal of surface conditions since they live in the shallow mixed layer. If there is a significant amount of planktonic foraminifera contributing to the bulk sediment, then this would maybe provide a mixed water column signal due to different species living at different depths through the upper 500 m. Reghellin et al. 2015 (in review) present a theoretical profile of the carbonate particle size distribution for bulk sediment but it is not supported by observations. It shows grain size abundance peaks that reflect dominance by coccolith carbonate (0-10 µm) and decreasing contributions from planktonic foraminifera fragments (a peak centered at 38 µm) and planktonic and benthic foraminifera (~>60 µm).

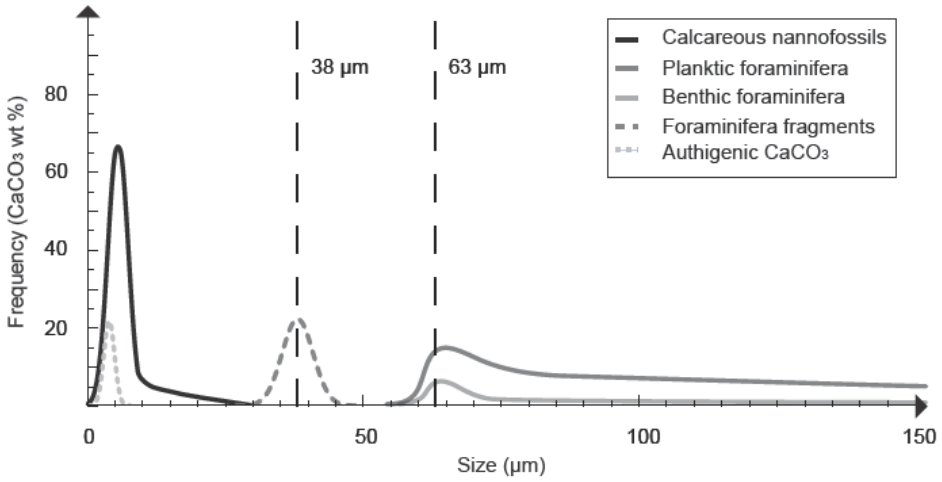

Figure 1; Theoretical profile showing particle size distributions of different marine organisms (Reghellin, et al., in review, 2015)

Studies concerning $CaCO_3$ distributions were carried out on three different deep sea sites from different ocean basins which will enable comparison. The IODP/ODP Sites that were compared are Leg 321 Site U1338 (Equatorial Pacific), Leg 154 Site 926 (Equatorial Atlantic) and Leg 121 Site 756 (Indian Ocean).

Particle-size distribution profiles were obtained for both bulk and residual sediment samples (acid treated to remove the carbonate component), which could then be subtracted from each other, providing information and a specific insight into the carbonate particle size distribution of the different samples. The final data obtained from grain-size analysis on the sediment samples could probably be used as an additional source of information for paleoceanographic interpretations (Reghellin. D.) of $\delta^{13}C$ and $\delta^{18}O$ of bulk coarse >63 um and fine <63 um fraction $CaCO_3$, which have been separated for isotopic analysis.

The use of stable isotopes in bulk sediment for paleoceanographic study is useful for the Equatorial Pacific where Site U1338 lies for two reasons. First, Site U1338 lies at a water depth of 4200m and sea floor sediments from much of the Cenozoic contain little $CaCO_3$ because they are close to the lysocline/CCD below which carbonate microfossils dissolve (Reghellin, et al., in review, 2015). At the present time the CCD in the Pacific Ocean is about 4200 – 4500 m. Second, bulk stable isotope analysis only requires small volumes of sample, in contrast to foraminifers that require a more extensive sample-preparation (sieving, manual picking etc.). Foraminiferal preservation is very poor at Site U1338 and this is related to low $CaCO_3$ content of sediment (LaMontage, et al., 1996; Lalicata and Lea, 2011). A rather central disadvantage when considering bulk stable isotope analysis, is the uncertainty when it comes to interpreting the results in terms of different water masses because of the multiple stable isotope signals ($\delta^{13}C$ & $\delta^{18}O$) that are recorded by all the different carbonate particles that make up the bulk (Reghellin, et al., 2015).

Questions

The principal questions that I addressed in this project;

- *How do bulk $CaCO_3$ grain size profiles vary over time (I.e. down core) and between different tropical oceanic settings?*
- *What grain size-classes are dominant?*
- *What can this tell us about the contribution of nannofossil (surface living planktonic algae) and planktonic foraminifera (protistan heterotrophic plankton that live in a wider range of depths in the water column) to the bulk?*

Experimental analysis has not been performed on this before in our department. For this reason, the project was developed with the intention of answering these questions by experimenting with the laser particle analyzer at Stockholm University IGV. Some problems were experienced during the process but some interesting results were obtained that are presented and interpreted below.

Oceanographic and sedimentary setting of the study sites

The sites were picked based on contrasting properties/factors corresponding to lithology, particle size spectra and ocean environments. Site U1338 from the EEP is one of the sites studied by Daniele Reghellin and information from here with respect to the questions listed above, would be useful to his studies of Neogene paleoceanography. The other two sites (926 and 756) represent different ocean environments from tropical (i.e. low latitude environments) known to have very different sediment compositions and particle size spectra, thus providing useful end members for comparison with the Eastern Equatorial Pacific.

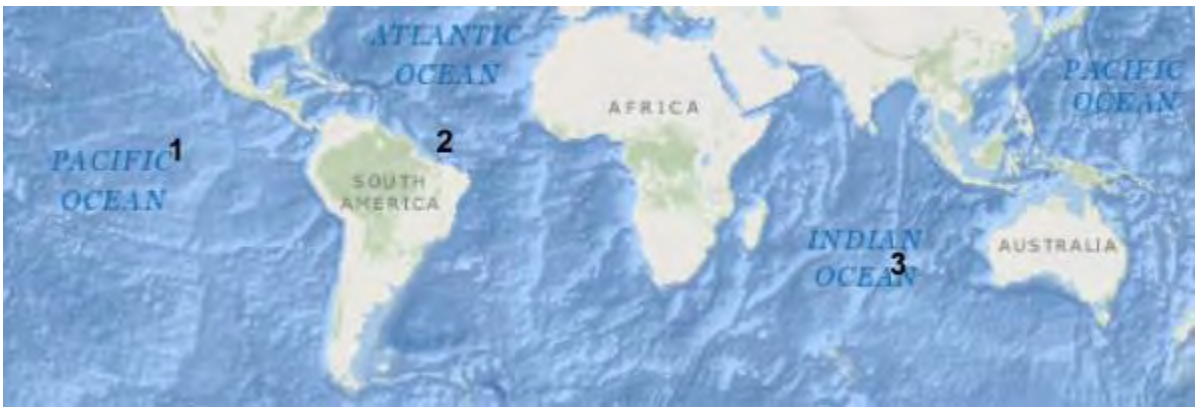

Figure 2; Worldmap produced in ArcMap showing the locations of the sites. (1) Site U1338 (2) Site 926 (3) Site 756

IODP Leg 321 Site U1338

Oceanography

Integrated Ocean Drilling Project (IODP) Site U1338 is located in the Eastern Equatorial Pacific between 2°30.47'N, 117°58.18'W at a water depth of 4200 m below sea level (Pälike, et al., 2010). The site is lying on 18 Ma crust in the area north of the Galapagos Fracture Zone. The topography is highest to the south and sloping down to the north-northwest and the sloping characteristic is synonymous with an abyssal hill.

The site was drilled uphill and at good distance away from a close by seamount (25km away) to avoid turbidites which were found at the nearby Sites of U1331 & U1335. Sediment thickness is 402m of pelagic type, and the site has through time been located within the direct influence of the southeast trade-wind belt and should therefore display the highest amount of windblown dust when taking all the PEAT Sites into contention (Pälike, et al., 2010). PEAT stands for Pacific Equatorial Age Transect and it was a drilling program designed to gain understanding about the paleo-Pacific Ocean and its evolution. Another goal of the PEAT program was to collect undisturbed sediments in order to produce a record of the paleo-environment of the Eastern Equatorial Pacific (Lyle, et al., 2010).

The oceanic conditions of the surrounding area are characterized by a high primary productivity due to the great input of solar radiation that is absorbed in the Eastern Equatorial Pacific (EEP) area (Lyle, et al. 2010) and a wind-driven upwelling that brings cold and nutrient rich waters to the surface. These cold waters are initially derived from the sinking of cold and dense mid-to high latitude surface waters in the southern and northern hemispheres (Lawrence, et al., 2006).

The trade winds drive surface water to either side of the equator due to the Coriolis Effect and cold nutrient rich waters can then come up through upwelling. This contributes to an enhanced supplement of nutrients and consequently higher rates of primary production**.** Since the depth of the thermocline has a relation to the wind, it controls the nutrient supply and therefore the biological production**.** The South Equatorial Current (SEC) is a trade wind-driven current which brings an open-ocean upwelling system with it (Pennington, et al., 2006).

Sediments

Sediments in the EEP is mainly comprised of biogenic carbonate, such as coccoliths (calcareous nannofossils) and foraminifera, but also biogenic opal with a small amount of clay (Frenz et al., 2005; Stoll et., al 2000; Romero, 2013). The biogenic opal is mainly composed of diatoms, but also radiolarians that have rather high growth rates in the euphotic zone under upwelling conditions. One factor that enhances the concentration of silica is the eastward shoaling of the nutricline. To explain further, the trade winds pushes surface waters in the EEP towards the west part of the ocean creating higher temperatures and sea surface levels. At the Eastern end of the basin, the thermocline will be tilted up to the west, followed by the nutricline, allowing nutrient-rich cold waters to well up to the surface (Krause,

et al., 2011). The linear sedimentation rate has decreased from about 29 cm/k.y. in the Miocene to about 13 cm/k.y. in the Pliocene-Pleistocene.

Lithostratigraphy

The four Holes U1338 A-D offer a 415 m sediment sequence of nannofossil ooze with varying concentrations of diatoms and radiolarians which overlie the seafloor basalt. The sequence is divided into three lithological units. In this grain-size analysis project, the focus will be on cores within Unit 1 which is of interest. This unit has a thickness of 50 meters and contains a sediment record from middle Pliocene to Pleistocene. Its composition is characterized by calcareous nannofossil ooze, diatom nannofossil ooze and radiolarian nannofossil ooze. Calcite grains with a size of <5µm are abundant in Unit 1 (Pälike, et al., 2010). In general, the nannofossils have a moderate preservation but in some intervals the preservation is good to poor. Planktonic foraminifera vary greatly in abundance from rare to abundant while the preservation is moderate to good throughout the sedimentary succession. Benthic foraminifera appear with continuity with generally good preservation (Pälike, et al., 2010).

ODP Leg 154 Site 926

Oceanography

Ocean Drilling Program (ODP) Site 926 is located on the southwestern part of the Ceara Rise (3°43.130'N, 42°54.508'W) at a depth of 3598 m above the present-day lysocline. It is the southernmost site drilled as a part of a depth transect on the Ceara Rise (Curry, et al., 1995). The surface water overlying the rise is characterized by equatorial oceanic conditions. Surface water has a mean annual temperature of 27˚C while also displaying low concentrations of nutrients since barely being affected by upwelling. This in turn leads to low productivity and the closeness to the Amazon River elevates the sedimentation rates (Curry and Cullen, 1997). The Amazon River has its source in the Andes (Heinrich and Zonneveld, 2013).

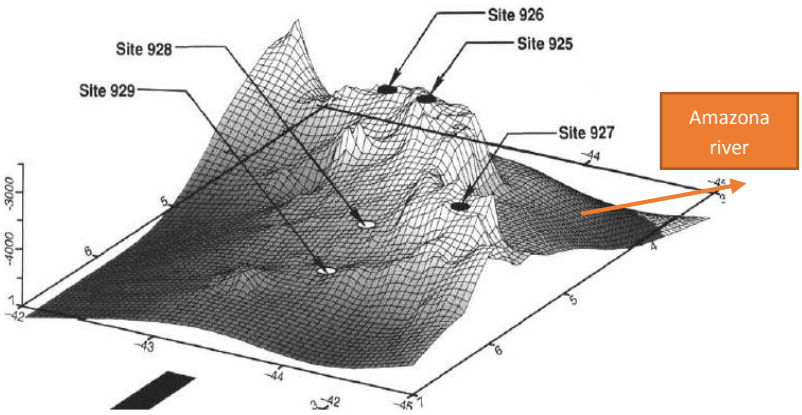

Figure 3; showing the bathymetry of site 926 (Curry W.B., et al 1995).

The Ceara Rise is a bathymetric high stretching between the depth intervals of 3000-4500 m and lies in the western Equatorial Atlantic Ocean and more specifically northeastward of the Amazon delta off the Brazilian coast, (Gibbs, et al., 2004). It was formed at the Mid-Atlantic Ridge around 80 m.y. years ago and it is moving westward and in some extent northwards at the same time. (Kumar and Embley, 1977). The Amazon Cone is a deep-sea fan that stretches from the continental shelf to abyssal depth and it's

fed by the Amazon River which discharges approximately 400 million tons of sediment each year (Kumar and Embley, 1977).

The NADW (North Atlantic Deep Water) and AABW (Antarctic Bottom Water) are two deep water currents flowing in the Ceara Rise area (Curry and Cullen, 1997). The NADW is directly influencing the Ceara Rise, running over the seafloor above the present day lysocline, having a southeastward flow path derived from northern latitudes (Gibbs, et al., 2004), whereas the latter one (AABW) flows northward having its source in the Antarctic region. Since the AABW is very dense, it flows on the deepest parts of the area and has played a significant role in the distribution of sediments. These two currents meet and mix in the 'mixing zone' (region between 4000-4500m) where the Ceara Rise is situated, some 800 km away from the Amazon River outlet (Kumar and Embley, 1977).

Figure 4; The study area is seen (Curry and Cullen, 1997)

Sediments

The sediments recovered from the Ceara Rise are represented by calcareous microfossils and terrigenous material, that latter being nearly fully composed of weathered material coming from the South American continent (Heinrich and Zonneveld, 2013) and being further transported into the equatorial Atlantic by the Amazon River which is the main source of terrigenous sediments and has been so since Miocene-time (Kumar and Embley, 1977). There is almost a total absence of organic carbon which could be associated with the long distance away from the river mouth but also due to the low amount of nutrients in the surface waters. The surface waters show small seasonal variability due to the equatorial location and the input of terrigenous material generates higher sedimentation rates than usually observed in regions with such low nutrient surface waters (Heinrich and Zonneveld, 2013). The preservation of carbonate components is generally very good. Since the last 16 m.y. sedimentation rates have progressively increased from around 12 cm/k.y. in the middle Miocene to about 33 cm/k.y. during Pleistocene. The increasing input of terrigenous material is related to the Amazon River. During the Miocene, episodes of severe dissolution caused the lysocline to shoal to depths shallower than 3600m, reducing sedimentation rates at site 926. The lysocline in the equatorial Atlantic remained well below 3600 m from early Pliocene to Holocene. (Curry and Cullen, 1997)

Lithostratigraphy

The majority of Site 926 sediment is made up of carbonate ooze, nannofossils and clay with foraminifers. The samples chosen are from Hole C and cores 1H-11H + 19H, where the core-interval of 1H-11H span within lithological Unit 1 (Pliocene - Pleistocene) at a depth-interval of 0-110 mbsf and the latter core (19H) comes from Lithological unit 2 (Early Late Miocene, approximately 175 m of depth) (Curry, et al., 1995).

ODP Leg 121 Site 756

Samples from ODP Leg 154 Site 756C provided a third tropical site for comparison. The site is located in the Southern Indian Ocean (27°21.253'S, 87°35.890'E) at a water depth of 1515.8 m. It lies on a sediment-covered area 10 km east of the crest of Ninetyeast Ridge which is a big north-south lineament. The corresponding ridge axis has a relief varying between 1500 – 3000m and a length ranging between 5000m while it is also covered by sediments from the Bengal fan. It is approximately 200km wide. The terrain of the location is uneven. Several peaks close to the site on the southern end of Ninetyeast ridge rises to water depths of 750 m. A fault with a 500 m vertical throw forms the southeastern edge of the bench.

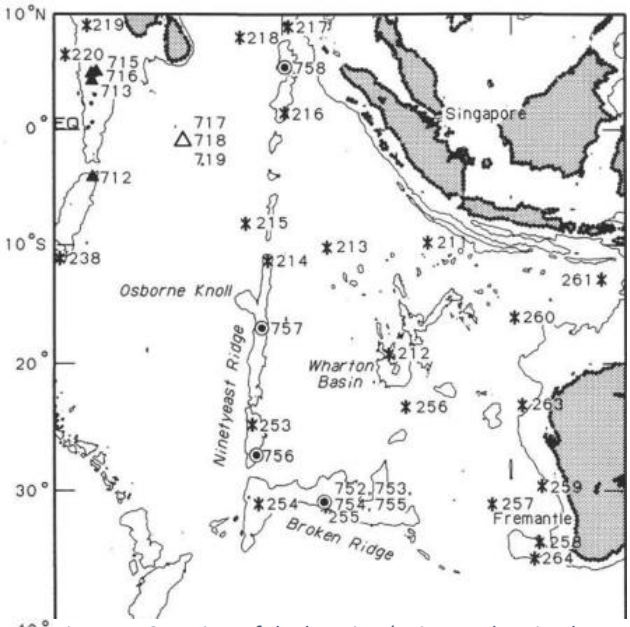

Figure 5; Overview of the location (Peirce and Weissel, et al., 1989).

From another perspective, Ninetyeast Ridge is located between the great deserts of Africa and Australia and it should therefore obtain a rather robust supply of dust, (Peirce and Weissel, et al., 1989).

Linear sedimentation rates for Site 756 lies around 0.36 cm/1000 yr. The rates were at 0.2 cm/1000 yr in the Oligocene and then rising to a high of 0.4 cm/1000 yr. in the Eocene and through the Miocene. The increase in grain size and the lower sedimentation rate during the Oligocene may indicate an increase in sorting at that time. The five samples picked from this site are from lithological unit 1A with an age of early Oligocene. This unit should be dominated by nannofossils with foraminifers, (Peirce and Weissel, et al., 1989).

Methods

Sample preparation

Samples from three different sites were identified and chosen for this project. Site U1338 lies in the equatorial Pacific while the other two are located in the Atlantic Ocean (Site 926) and Indian Ocean (Site 756). This was done in order to provide data for comparing profiles of carbonate grain size distribution. Site 756 was initially chosen with the intension of providing test-samples in order to get familiar with the steps that comprise the method of work for this project.

Five samples were chosen from Site 756. Ten samples each were chosen from Sites U1338 and 926. For Site U1338, two samples were chosen from the same cores but from different sections. This was done out of interest, since the samples showed visual contrasts in color with one being darker/lighter than the

other. This visual difference in color would presumably be related to a compositional difference with the lighter samples being richer in carbonate and the darker in siliceous and terrigenous material. The small plugs containing the samples have a volume of material corresponding to 10 cubic centimeters before freeze drying.

The samples were poked out from the plugs and split into two halves, each making up approximately 5 cubic centimeters of material. One half was saved for acidification (carbonate removal) and the other half for bulk sample analysis. The time was not enough for freeze drying and weighing the samples, however this is something that should be done in the future when these experiments are repeated.

Site U1338

Table 1; An overview of parameters including sample ID, age, lithology, sample description, depths (mbsf) and $CaCO_3$ contents (Pälike, et al. 2010).

Sample ID	**Age**	**Lithology**	Description	**Depth (**mbsf)
321-U1338B-1H-2W 40-42	Pleistocene	Nannofossil ooze, diatoms and calcite, oxides + siliceous-ooze (Diatom ooze)	Pale brown	1,9 m
321-U1338B-1H-2W 89-90	Pleistocene	Nannofossil ooze, diatoms and calcite, oxide + siliceous ooze (Diatom ooze)	Pale brown	2,4 m
321-U1338B-2H-4W 90-92	Pleistocene	Nannofossil ooze, calcite and foraminiferas + siliceous-ooze (diatom ooze)	Light olive brown	12,5 m
321-U1338B-2H-6W 100-102	Pleistocene	Nannofossil ooze, calcite and foraminiferas + siliceous-ooze (Diatom ooze)	Greenish grey	16 m
321-U1338B-3H-4W 89-90	Pleistocene	Nannofossil ooze + radiolarians & diatoms	Greenish gray	22 m
321-U1338B-3H-7W 60-62	Pleistocene	Nannofossil ooze + radiolarians & diatoms	Greenish gray	26,5 m
321-U1338A-4H-4W 20-22	Pliocene	Nannofossil ooze, calcite, radiolarians, diatoms	Greenish gray	31,5 m
321-U1338A-4H-5W 70-72	Pliocene	Nannofossil ooze, calcite, radiolarians, diatoms	Greenish grey	33,5 m
321-U1338C-5H-1W 130-132	Pliocene	Diatom nannofossil ooze + radiolarians + calcite	Greenish gray (light)	37,5 m
321-U1338C-5H-2W 10-12	Pliocene	Diatom nannofossil ooze + radiolarians + calcite	Greenish gray (light)	37,6 -37,8 m

Site 926

Table 2; An overview of parameters including sample ID, age, lithology, description, depths (mbsf) and $CaCO_3$ contents (Curry, et al., 1995).

Sample ID	Age	Lithology (IODP)	Description (IODP)	Depth (mbsf)
154-926C-1H-06 40-41	Pleistocene	Clay with nannofossils, nannofossil clay mixed sediment with foraminifers, **and** clayey nannofossil ooze with foraminifers.	Brownish gray	8 m
154-926C-2H-01 120-121	Pleistocene	Nannofossil clay mixed sediment with foraminifers	Light grayish brrown	11 m
154-926C-3H-06 120-121	Pleistocene	Clay with nannofossils **and** nannofossil clay mixed sediment with foraminifers.	Light brownish gray	28 m
154-926C-4H-04 120-121	Pleistocene	Nannofossil Clay	Grayish brown	34,5 m
154-926C-5H-03 40-41	Pleistocene	Nannofossil Clay and Nannofossil ooze with clay and foraminifers	Light grayish brown	39 m
154-926C-7H-06 40-41	Pliocene	Clayey nannofossil ooze with foraminifers a**nd** nannofossil clay mixed sediment with foraminifers	Light gray & Light grayish brown	65,5 m
154-926C-8H-06 40-41	Pliocene	Nannofossil clay mixed sediment and Clayey nannofossil ooze with foraminifers	Light grayish brown	75 m
154-926C-9H-06 120-121	Pliocene	Clayey nannofossil ooze with foraminifers and Nannofossil clay mixed sediment with foraminifers	Light gray & light grayish brown	85 m
154-926C-11H-02 120-121	Pliocene	Foraminifer nannofossil ooze with clay and Clayey nannofossil ooze with foraminifers	Light gray & light grayish brown	98 m
154-926C-19H-01 40-41	Late Miocene	Clayey nannofossil ooze	Light gray	172 m

Site 756

Table 3; An overview of parameters including sample ID, age, lithology, sample description, depths (mbsf) and $CaCO_3$ contents. (Peirce and Weissel, et al., 1989)

Sample ID (ODP)	Age (DOP)	Lithology (ODP)	Description (ODP)	Depth (mbsf)
121-U756C-5X-06-WW 40-42	Early Oligocene	Nannofossil ooze with foraminifers	White to very pale brown	114.4 m
121-U756C-5X-06-WW 60-62	Early Oligocene	Nannofossil ooze with foraminifers	White to very pale brown	114.6 m
121-U756C-5X-06-WW 78.5-80.5	Early Oligocene	Nannofossil ooze with foraminifers	White to very pale brown	114.8 m
121-U756C-5X-06-WW 79-81	Early Oligocene	Nannofossil ooze with foraminifers	White to very pale brown	114.9 m
121-U756C-5X-06-WW 100-102	Early Oligocene	Nannofossil ooze with foraminifers	White to very pale brown	115 m

Carbonate Removal

Site 756 (Test Samples)

The first step in the procedures for removal of carbonate was to produce buffered acetic acid based on the following formula: 82g of Sodium Acetate, 25 ml of Glacial Acetic Acid, 1 liter of DI H_2O (Buhrke, et al., 1998). The first step was performed by pouring 5 liters of deionized water in to a plastic can and then adding 125 ml of glacial acetic acid. The next step was to weigh up 82 x 5 g of sodium acetate that was added into the liquid mixture. The procedure was concluded by shaking the bottle well in order for the ingredients to mix up well. The adding of the different constituents were performed under the fume hood with regard to safety while also using protective safety equipment such as gloves, glasses and lab coat.

Preparation of samples

The plastic bags of the five dried samples from Site 756 were labelled 1-5 and gently homogenized. Half of these (approximately 5 cc) were put in five 250 ml Erlenmeyer flasks which were also labeled respective to the samples to avoid confusion. 150 ml of buffered acetic acid solution were slowly added into each flask. A stopper with a hole was then inserted into each flask. Lastly, the E-flasks were shaken before inserting them into the shaker table at a speed of 5.

The samples were agitated for 2 hours on the shaker table and then taken off to allow the sediment to settle for approximately one hour. At this point most of the sediment had settled pretty quickly but the solution would still be a bit cloudy which is not optimal. The next step was to siphon off the supernatant (solution consisting the dissolved carbonate) over the sink, using a vacuum tube under running water while gently tipping the beaker to the side which facilitates the procedure and minimizes the loss of sediment. It was necessary to be gentle with the siphon-tube so one does not soak up any of the settled sediment.

These processes were repeated 6 times (6 washes) on the samples from Site 756 until there were no bubbles/fizzing left after insertion of buffered acetic acid which indicates that the samples should be carbonate-free. Lastly the non-reactive residues were washed twice with deionized water by adding an aliquot of 150 ml while using the exact same method as the acidic washes and this time letting the flasks filled with deionized water to settle on the countertop until the solution was totally clear.

The same method was used for Site 926 except that 15 times washes with buffered acetic acid and twice with deionized water were required.

A small change in the approach was required for Site U1338 samples. The halves (5CC) of the five respective samples that were going to be treated with acid, were prepared by homogenizing first a mortar and pestle in order to optimize the acidification process, making it more effective by gaining time and minimizing the volume of buffered acetic required to dissolve the carbonate; There was a concern

that the non-carbonate particles might also become mechanically and chemically attacked and potentially break up.

Grain size analysis

Mastersizer 3000 (Malvern Instruments)

The Malvern Instrument works by measuring the intensity of light scattering as a laser beam goes through a dispersed sample of particles. The particles passes through the measurement area of the laser. The particles will be illuminated by the laser beam which bounces off the different particle sizes. If it is a large particle, the beam will create a narrow angle while if it is a small particle, a large angle will be produced. The detectors then measure the light intensity that is scattered by the particles over a big range of angles. The instrument has to be and powered up for approximately 30 before measurements can be made.

The tap for deionized water on the wall behind the instrument has to be opened to let the water flow out and then start the program on the computer while choosing the manual measurement with appropriate settings such as dispersant, amount of measurements (5), material-properties, type of cleaning(manual), ultrasound-settings (3 min) and obscuration range. The detectors of the instrument are controlled by making sure that detector 1 displays <100 and detector 20 <20 which demonstrates that the system is clean. If not, then a cleaning is necessary.

Procedure

The same approach was executed for running both the bulk samples and the ones treated with acid. After starting the machine and letting it warm up for 30 min, the sample chamber of the instrument is cleaned through the program while also giving it a hand manually by spraying deionized water from a plastic bottle to make sure that it is totally clean and free of eventual particles. The Hydro LV can will then be automatically refilled with 600 ml of deionized water. Afterwards the stirrer has to be enabled at full speed (3500 rpm) and then adding 3 ml of 10% sodiumhexametaphosphate (dispersant which will give more stable measurement values) into the deionized water in the Hydro-LV which will give a concentration of 0.05%. Next, initialize the instrument, check the detectors and measure the background. These steps are controlled through the computer interface.

The next step was to add the sample, ensuring that it was well mixed.

The sample was then ultrasonicated for 3 minutes, which helps disaggregate the particles to avoid aggregates. Under this time-frame the obscuration gradually decreased for the bulk-samples. A test was made first to see how much sediment was needed in order to achieve a good obscuration after the 3 minutes. When the ultrasound stops, the analysis was started using the ‘measure sample’ command. The instrument performed 5 measurements over 3,5 minutes. These steps were repeated for each

sample. The same procedure was used for the acidified samples. For these samples with small sediment volumes it was necessary to strongly mix the sample with a plastic dropper before inserting into the sample chamber, in order to get a representative sample with all the grain-sizes included. One replicate was done of each sample to get the precision.

Laser obscuration

'Laser obscuration' is how much of the laser/light that is prevented by the particles and in this way one can know the quantity of the concentration of the particle sizes. For example, if a straight line is obtained along the base of the grain-size profile it means that all the light is going through and consequently there are no particles obscuring the laser beam. A stream of particles passes between the light source and a detector. It illuminates the individual particles in the water which results in a blockage of light on the detector. This light blockage is termed 'obscuration'. The detector measures this reduction in light intensity a signal to determine the size of the particle is processed.

A high laser obscurity gives a better representation of the sample but there is a risk for multiple scattering. Too low laser obscuration results in that not enough particles are being measured in order to obtain a representative estimation of the samples grain size distribution. It is observed as high standard deviations of especially the 90^{th} percentile (Dv90).

Smear slide preparation and analysis

Smear slides were performed for the residual sediment. The first step was to put a small drop of sediment (diluted in deionized water) on a microscope glass and placing it on a hot plate to dry. Afterwards small grains of acaye were inserted on the sediment followed by a cover glass. Putting some force with a spatula was necessary in order to remove bubbles.

Results

The results are organized site by site. Individual bulk and residual grain size distribution profiles (figures 5-7) from the particle analyzer are presented for each site to show the modes. Tables showing the median grain size are also presented. Microscope observations of the dominant sedimentological / and microfossil components observed in smear slides are presented in accompanying tables. The laser analyzer treats the bulk and residual as if they make up 100% of the sample. Comparing bulk and residual therefore is not possible using these first plots because accurate information about the exact volume of the residual with respect to bulk is lacking. The profiles then show the grain size distribution in each case and only the relative proportions of the residual.

Attempts to scale the residual and extract the actual volumetric bulk/residual relationship are made below in the discussion and presented in figures (9-11)

IODP Site U1338

Bulk

Table 5; Median grain size for 10 bulk samples from site U1338.				
Order by depth	**Depth (mbsf)**	**Sample ID**	**Sample Name**	**Dx (50) (µm)**
1	1,9	321-U1338B-1H-2W 40-42	Average of '1'	26,1
2	2,4	321-U1338B-1H-2W 89-90	Average of '2'	25,7
3	12,5	321-U1338B-2H-4W 90-92	Average of '3'	33,1
4	16	321-U1338B-2H-6W 100-102	Average of '4'	13,8
5	22	321-U1338B-3H-4W 89-90	Average of '5'	15,1
6	26,5	321-U1338B-3H-7W 60-62	Average of '6'	15,3
7	31,5	321-U1338A-4H-4W 20-22	Average of '7'	13,9
8	33,5	321-U1338A-4H-5W 70-72	Average of '8'	14,0
9	37,5	321-U1338C-5H-1W 130-132	Average of '9'	18,3
10	37,6 -37,8	321-U1338C-5H-2W 10-12	Average of '10'	18,4

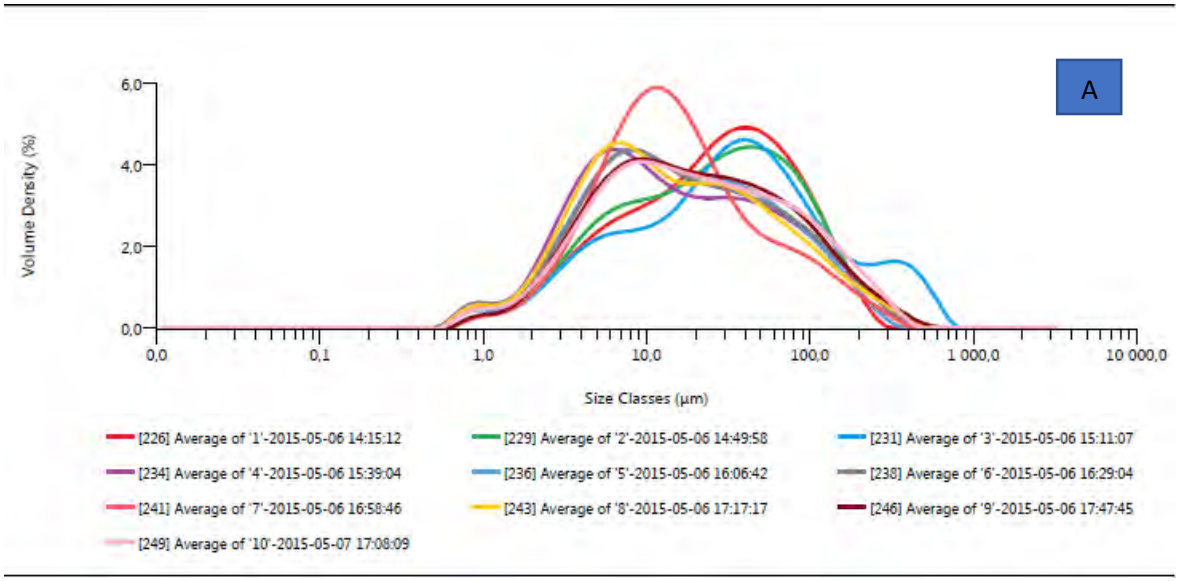

Figure 6A; Bulk grain size distribution for 10 samples from Site U1338 organized by increasing depth in core. The axis are volume % against size classes (µm). The x-axis is logarithmic scale.

The bulk sediment particle size distribution profiles from U1338 (fig 6A) show modes at 0,8 µm, 5-8 µm, 10-15 µm, 30 µm, 40-50 µm, 90 µm and 400 µm. All of the samples have a similar mode around 0,8 µm. The sample profiles fall into two main clusters. Samples (2,4,6,9,10) peak between 5-8 µm, Sample (7) within 10-15 µm, Sample (10) at 30 µm and 90 µm whereas Sample (3) show a mode at 400 µm. Table 5 is presenting the median size class for the 10 bulk samples.

Residual

Table 6; Median grain size for 10 residual samples from Site U1338.

Order by depth	Depth (mbsf)	Sample ID	Sample Name	Dx (50) (µm)
1	1,9	321-U1338B-1H-2W 40-42	Average of '1 CF'	29,7
2	2,4	321-U1338B-1H-2W 89-90	Average of '2 CF'	24,9
3	12,5	321-U1338B-2H-4W 90-92	Average of '3 CF'	30,1
4	16	321-U1338B-2H-6W 100-102	Average of '4 CF'	16,3
5	22	321-U1338B-3H-4W 89-90	Average of '5 CF'	21,1
6	26,5	321-U1338B-3H-7W 60-62	Average of '6 CF'	19,0
7	31,5	321-U1338A-4H-4W 20-22	Average of '7 CF'	12,8
8	33,5	321-U1338A-4H-5W 70-72	Average of '8 CF'	15,9
9	37,5	321-U1338C-5H-1W 130-132	Average of '9 CF'	16,6
10	37,6 -37,8	321-U1338C-5H-2W 10-12	Average of '10 CF'	17,7

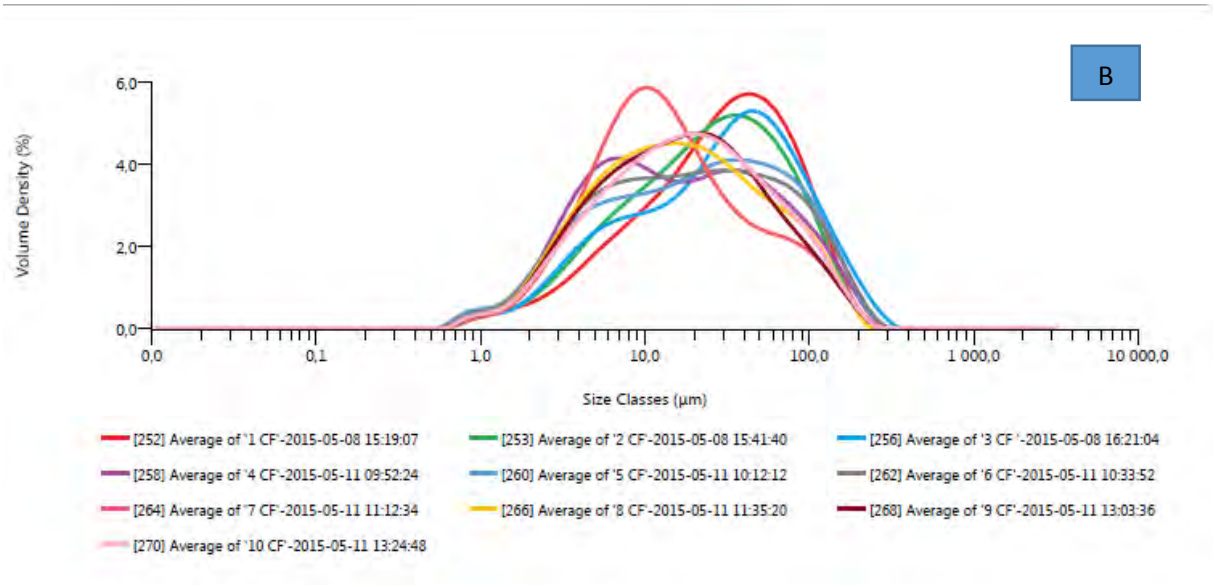

Figure 6B; Residual grain size distribution for 10 samples from Site U1338 organized by increasing depth in core. The axis are volume % against size classes (µm). The x-axis is logarithmic scale.

The de-carbonated residual samples (fig 6B) have similar grain size profile shapes and modes to the bulk. The profiles show a mode between 5-8 µm for samples (4,6,5). Sample (7) peak at 10 µm and 90 µm, sample (8) at 15 µm, Samples (9, 10) at 25 µm, samples (1,2,3,4,5) within 35-50 µm. Table 6 shows the median size class for the residual samples. The rather similar profile shapes and the general increasing volume for the residual sediment samples compared to the bulk samples is not what is expected. This has to do with the incorrect bulk:residual ratio (100% : 100%). This is a limitation of the laser analyzer that will be mentioned and discussed further.

Smear Slides

Table 7; Qualitative records of the dominant sedimentary residual material observed in the smear slides, highlighting my own observations (this study) with respect to published IODP references.

Sample ID	Dominant lithological components (IODP)	Description of smear slide (this study)
321-U1338B-1H-2W 40-42	Calcareous nannofossil ooze with **Diatoms** and radiolarians.	Approximately the same ratio between intact and fragmented diatoms. (Fe-oxides?). The diatoms are big.
321-U1338B-1H-2W 89-90	Calcareous nannofossil ooze with **Diatoms** and radiolarians.	More radiolarian than previous sample. A lot are intact. A lot of very small radiolarian fragments with a minor amount of intact ones.
321-U1338B-2H-4W 90-92	Nannofossil ooze with calcites and diatoms.	Approximately the same amount of diatoms as previous sample. Most diatom frustules are fragmented.
321-U1338B-2H-6W 100-102	Nannofossil ooze with diatoms, calcites and radiolarians.	Mostly diaoms + introduction of an elongated diatom species (needle-like).
321-U1338B-3H-4W 89-90	Nannofossil ooze with diatoms, calcites and radiolarians.	Fragmented radiolaria & diatoms. A lot of brown inclusions which could maybe be clays or Fe-oxides.
321-U1338B-3H-7W 60-62	Nannofossil ooze with diatoms, calcites and radiolarians.	Fragmented radiolaria and fragmented diatoms.
321-U1338A-4H-4W 20-22	Nannofossil ooze with calcites and radiolarians.	Fragmented radiolaria and a very high concentration of heavily fragmented large diatoms.
321-U1338A-4H-5W 70-72	Nannofossil ooze with calcites and radiolarians.	Heavily fragmented organisms.
321-U1338C-5H-1W 130-132	Nannofossil ooze with diatoms and radiolarians.	Heavily fragmented organisms.
321-U1338C-5H-2W 10-12	Nannofossil ooze with diatoms radiolarians.	Heavily fragmented orgaisms.

ODP 154 Site 926

Bulk

Table8; Median grain size for 10 bulk samples from Site 926.				
Order by depth	**depth**	**Sample ID**	**Sample Name**	**Dx (50) (µm)**
1	8 m	154-926C-1H-06 40-41	Average of '1'	3,80
2	11 m	154-926C-2H-01 120-121	Average of '2'	4,54
3	28 m	154-926C-3H-06 120-121	Average of '3'	44,0
4	34,5 m	154-926C-4H-04 120-121	Average of '4'	6,20
5	39 m	154-926C-5H-03 40-41	Average of '5'	26,7
6	65,5 m	154-926C-7H-06 40-41	Average of '6'	60,7
7	75 m	154-926C-8H-06 40-41	Average of '7'	5,47
8	85 m	154-926C-9H-06 120-121	Average of '8'	21,1
9	98 m	154-926C-11H-02 120-121	Average of '9'	17,0
10	172 m	154-926C-19H-01 40-41	Average of '10'	7,08

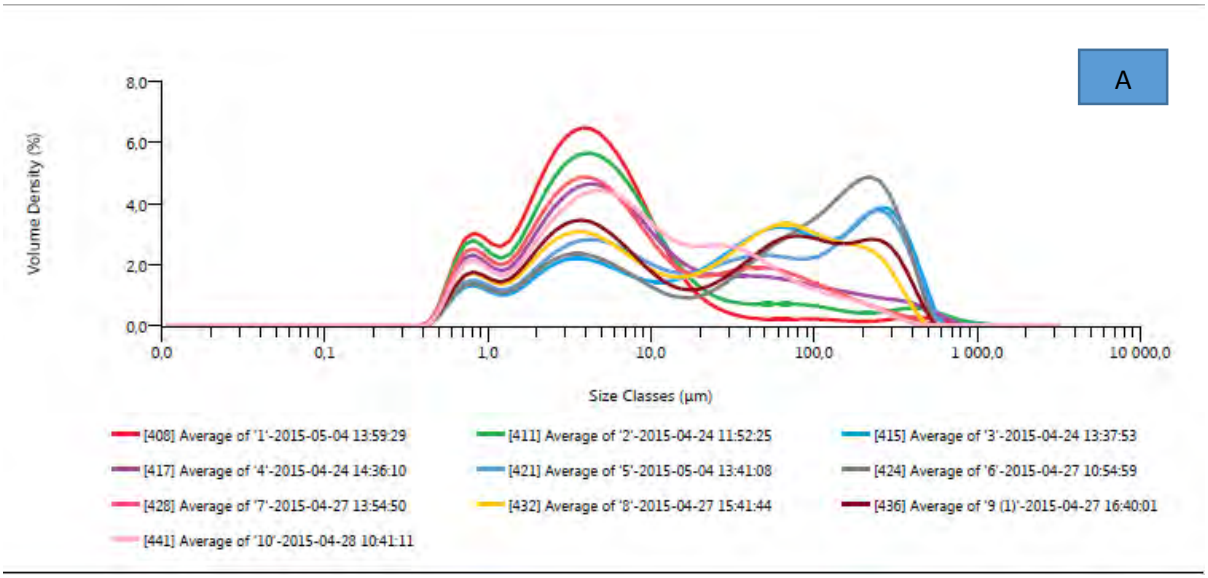

Figure 7A; Bulk grain size distribution for 10 samples from Site 926 organized by increasing depth in core. The axis are volume % against size classes (µm). The x-axis is logarithmic scale.

Bulk sediment particle size profiles from Site 926 show greater variability between its samples compared to Site U1338. Figure 7A is showing a modes at 0,8 µm, 3-5 µm, 30 µm, 60-80 µm and 200 µm-300 µm. All of the samples have a similar mode around 0,8 µm and 3-5 µm. Sample 10 is an exception peaking again at 30 µm. Samples (1,3,8,9) peak at between 60-80 µm whereas samples (3,5,6,9) peak again between the broad interval of 200-300 µm . Table 8 is presenting the median size class for the bulk samples.

Residual

Table 9; Median grain size for 10 residual samples from Site 926.				
Order by depth	**Depth (mbsf)**	**Sample ID**	**Sample Name**	**Dx (50) (µm)**
1	8 m	154-926C-1H-06 40-41	Average of '1'	3,80
2	11 m	154-926C-2H-01 120-121	Average of '2'	4,54
3	28 m	154-926C-3H-06 120-121	Average of '3'	44,0
4	34,5 m	154-926C-4H-04 120-121	Average of '4'	6,20
5	39 m	154-926C-5H-03 40-41	Average of '5'	26,7
6	65,5 m	154-926C-7H-06 40-41	Average of '6'	60,7
7	75 m	154-926C-8H-06 40-41	Average of '7'	5,47
8	85 m	154-926C-9H-06 120-121	Average of '8'	21,1
9	98 m	154-926C-11H-02 120-121	Average of '9'	17,0
10	172 m	154-926C-19H-01 40-41	Average of '10'	7,08

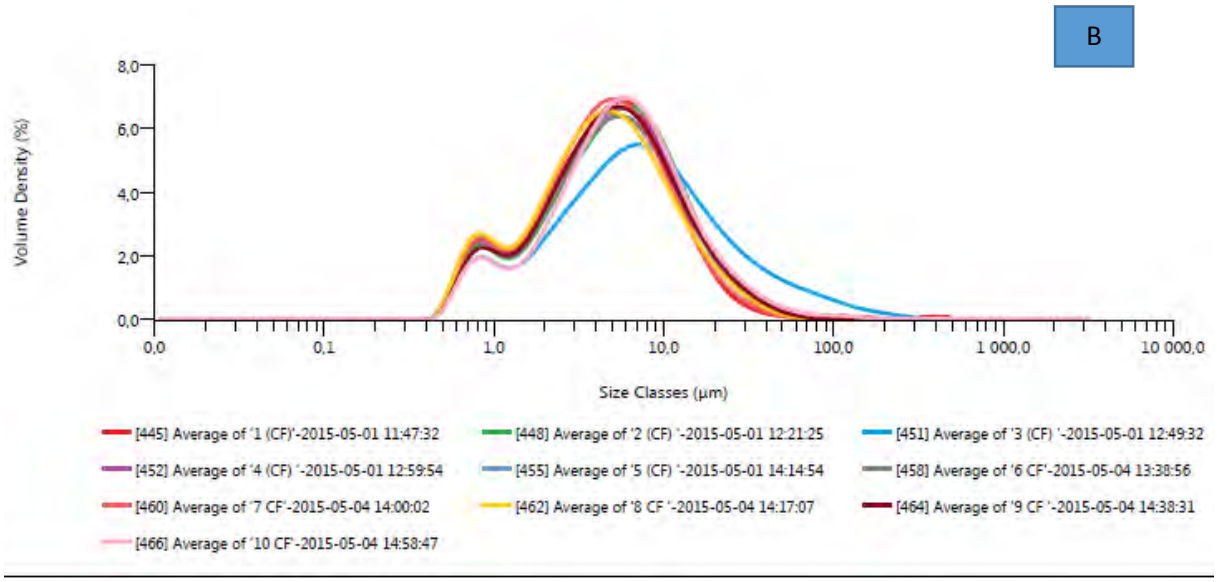

Figure 7B; Residual grain size distribution for 10 samples from Site 926 organized by increasing depth in core. The axis are volume % against size classes (µm). The x-axis is logarithmic scale.

The de-carbonated residual samples (Fig 7B) show a different pattern from the bulk profile (Fig 7A). The particle size distribution is very similar for all of the residual samples from Site 926 showing modes at 0,8 µm and within 4-7 µm. Sample 3 is somewhat of an anomaly, having a skewed peak around 8 µm. Table 9 is presenting the median size class for the residual samples.

Smear Slides

Table 10; Qualitative records of the dominant sedimentary residual material observed in the smear slides, highlighting my own observations (this study) with respect to published ODP references. All samples have the same lithology.

Sample ID	Dominant lithological components (IODP)	Description of smear slide (this study)
154-926C-1H-06 40-41 154-926C-2H-01 120-121 154-926C-3H-06 120-121 154-926C-4H-04 120-121 154-926C-5H-03 40-41 154-926C-7H-06 40-41 154-926C-8H-06 40-41 154-926C-9H-06 120-121 154-926C-11H-02 120-121 154-926C-19H-01 40-41	Nannofossils, clay, silt, sand.	Clay minerals dominant. Silt is present with minor amounts of sand.

ODP Site 756

Bulk

Table 11; Median grain size for 10 bulk samples from Site 756				
Order by depth	**Depth (mbsf)**	**Sample ID**	**Sample Name**	**Dx (50) (µm)**
1	114.4 m	121-U756C-5X-06-WW 40-42	Average of '1'	12,9
2	114.6 m	121-U756C-5X-06-WW 60-62	Average of '2'	32,9
3	114.8 m	121-U756C-5X-06-WW 78.5-80.5	Average of '3'	13,0
4	114.9 m	121-U756C-5X-06-WW 79-81	Average of '4'	29,6
5	115 m	121-U756C-5X-06-WW 100-102	Average of '5'	26,4

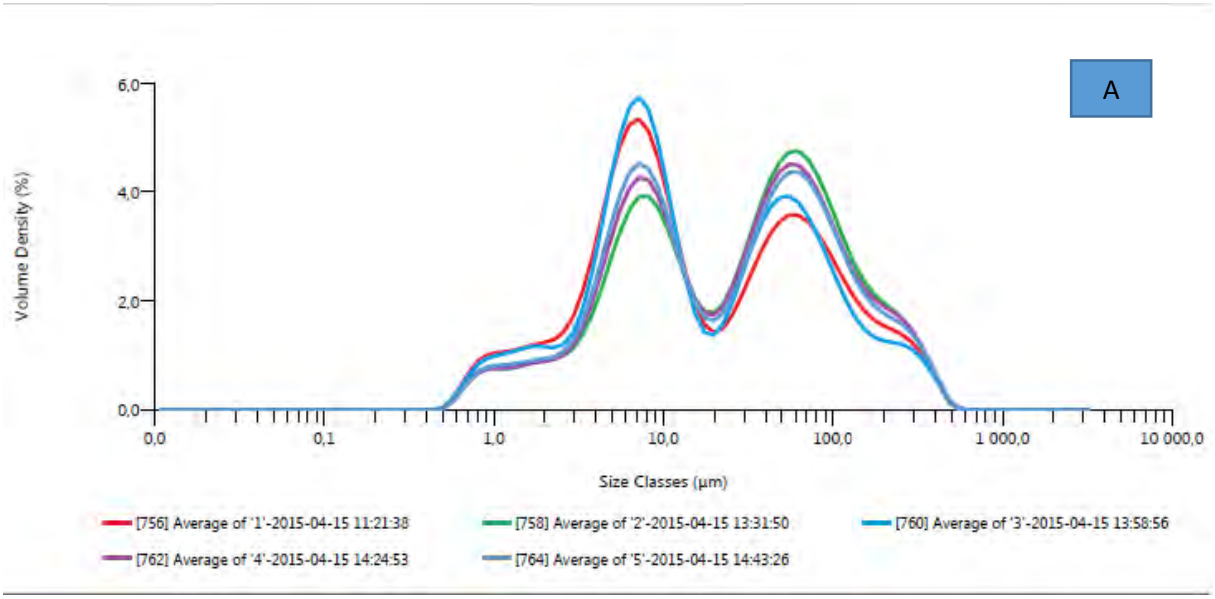

Figure 8A; Bulk grain size distribution for 10 samples from Site 756 organized by increasing depth in core. The axis are volume % against size classes (µm). The x-axis is logarithmic scale.

Bulk sediment particle size profiles (Figure 8A) from Site 756 are similar and show peaks at 1 µm, 6-8 µm, 50 – 70 µm and 300 µm for all of the samples. Table 11 is presenting the median size class for the 10 bulk samples. Sample 1 have a more skewed mode at 55 µm and sample 3 at 60 µm.

Residual

Table 12; Median grain size for 10 residual samples from Site 756				
Order by depth	**Depth (mbsf)**	**Sample ID**	**Sample Name**	**Dx (50) (µm)**
1	114.4 m	121-U756C-5X-06-WW 40-42	Average of '1 CF'	6,51
2	114.6 m	121-U756C-5X-06-WW 60-62	Average of '2 CF'	6,77
3	114.8 m	121-U756C-5X-06-WW 78.5-80.5	Average of '3 CF'	14,9
4	114.9 m	121-U756C-5X-06-WW 79-81	Average of '4 CF'	6,77
5	115 m	121-U756C-5X-06-WW 100-102	Average of '5 CF'	12,7

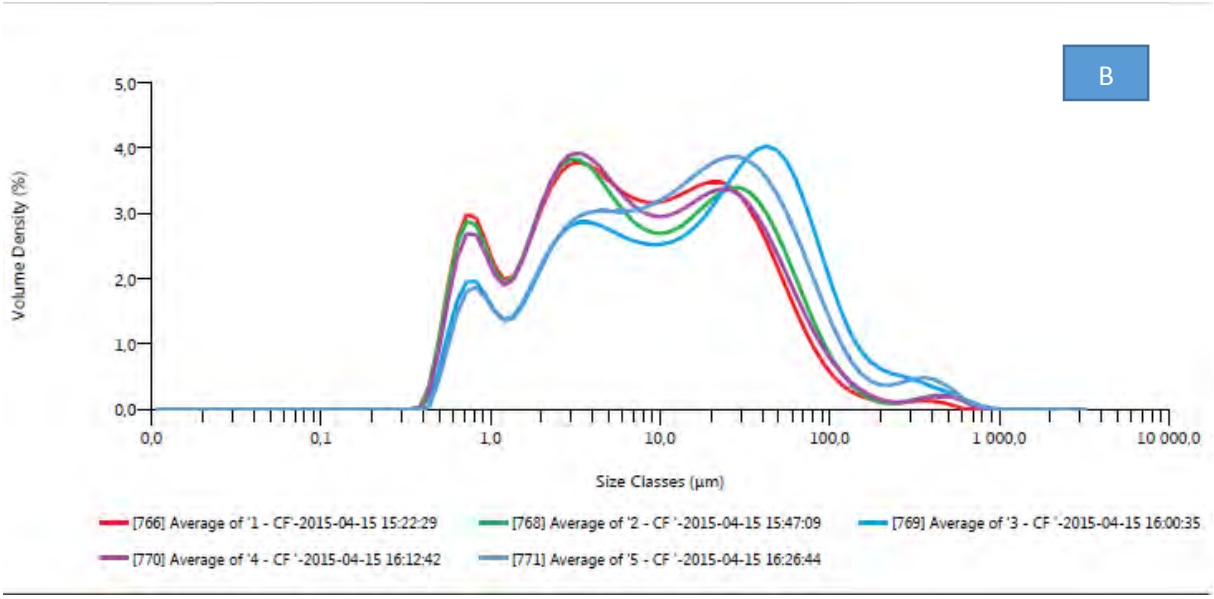

Figure 8B; residual rain size distribution for 10 samples from Site 756 organized by increasing depth in core. The axis are volume % against size classes (µm). The x-axis is logarithmic scale

Residual sediment particle size profiles (Figure 8B) from Site 756 are largely showing modes at 0,8 µm, 2,5-4 µm, 25 µm, 30 µm and 40-50 µm, with some variability between samples. All of the samples peak at about 0,8 µm and 2,5-4 µm with some variability between the samples. Sample 1 peak at 25 µm, Samples (2, 5) at 30 µm and sample 3 at 40-50 µm. Table 8 is presenting the median size class for the residual samples.

Smear slides

Table 13; Qualitative records of the dominant sedimentary residual material observed in the smear slides, highlighting my own observations (this study) with respect to published ODP references. All samples have the same lithology.

Sample ID	Dominant ithological components (ODP)	Description of smear slide (this study)
121-U756C-5X-06-WW 100-102 121-U756C-5X-06-WW 40-42 121-U756C-5X-06-WW 79-81 121-U756C-5X-06-WW 60-62 121-U756C-5X-06-WW 78.5-80.5	Nannofossil ooze, Clay, silt and sand	Mostly silt with minor amounts of clay and sand

Discussion

The primary interest in this project is the grain size distribution of bulk carbonate material because which is used to generate carbon and oxygen stable isotopic palaeoceanographic signals and it is necessary to improve knowledge of the kind of particles dominating this bulk sediment in different oceanic settings. To explore this further, the data have been re-plotted sample by sample to show the difference between bulk sediment versus non carbonate sediment (residual).

The grain size histograms (orange) (figures 9-11) present the residual sediment as bars within phi bins (converted to µm) and the blue curves represent the bulk. The logarithmic phi scale allows grain-size data to be expressed in units of equal value for the purpose of graphical plotting and statistical calculations (Boggs, 2011). An important limitation of the method used here is that the laser analyzer data outputs are all relative to the sample put in – i.e. the machine does not know that the acidified residual is a sub-fraction of another sample. Thus the raw data outputs show the residual grain size distribution spectra is 100% volume as the bulk, which makes little sense when presented visually. We do not know the exact ratio of the residual versus the bulk sediment since we did not weigh the sample before and after acidification. This we realized was an oversight but there was insufficient time to re-do the analysis with dried and weighed samples. From the experience of removing carbonate through acidification it is clear that there is typically a lot more carbonate than residual. In order to make a realistic view of the relationship between the bulk and residual and to make them more presentable visually, I have taken the average % carbonate content for the three sites from published measurements (Pälike, et al. 2010; Curry, et al., 1995; Peirce and Weissel, et al., 1989) and scaled the residual accordingly. The assumption is that all non-carbonate material, corresponding to our 'residual' makes up for the remainder of the sample. E.g. if the carbonate content is 60 % the residual must be 40%, thus the residual volumes are reduced by 40% (multiplied by 0.4). These orange bars have an approximate estimate of the properties. These profiles are presented in figures (9-11) and presented by depth, going from shallow to deep (sample 1-10 is referring to the order, going from right to left) for the different sites. One issue is that the carbonate concentration is an average measurement that is not from the samples used here, although nearby in the core.

Table 14; $CaCO_3$ values used to scale the residual samples for Site U1338 (Pälike, et al., 2010), Site 926 (Curry, et al., 1995) and Site 756 (Peirce and Weissel, et al., 1989).

Sample ID (U1338)	$CaCO_3$ % (U1338)	Sample ID (926)	$CaCO_3$ (%) (926)	Sample ID (756)	$CaCO_3$ (%) (756)
321-U1338B-1H-2W 40-42	77	154-926C-1H-06 40-41	35	121-U756C-5X-06-WW 40-42	94
321-U1338B-1H-2W 89-90	77	154-926C-2H-01 120-121	35	121-U756C-5X-06-WW 60-62	94
321-U1338B-2H-4W 90-92	80	154-926C-3H-06 120-121	35	121-U756C-5X-06-WW 78.5-80.5	94
321-U1338B-2H-6W 100-102	80	154-926C-4H-04 120-121	35	121-U756C-5X-06-WW 79-81	94
321-U1338B-3H-4W 89-90	60	154-926C-5H-03 40-41	42	121-U756C-5X-06-WW 100-102	94
321-U1338B-3H-7W 60-62	60	154-926C-7H-06 40-41	42		
321-U1338A-4H-4W 20-22	63	154-926C-8H-06 40-41	42		
321-U1338A-4H-5W 70-72	63	154-926C-9H-06 120-121	42		
321-U1338C-5H-1W 130-132	67	154-926C-11H-02 120-121	72		
321-U1338C-5H-2W 10-12	67	154-926C-19H-01 40-41	72		

Bulk and residual grain size distributions

Figure 1 in this thesis showed a theoretical grain size distribution for carbonate particles; fine grained nannofossils within 1-20 µm (peak at 5 µm), foraminiferal fragments within 30-40 µm (peak at 38 µm), planktonic and benthic foraminifera between 55 µm and higher grain sizes (peak at 63 µm). I will use the smear slides of the residual material (clay, silt, sand, diatoms and radiolarian) to qualitatively explain the contributions of the non-carbonate particles.

Site U1338

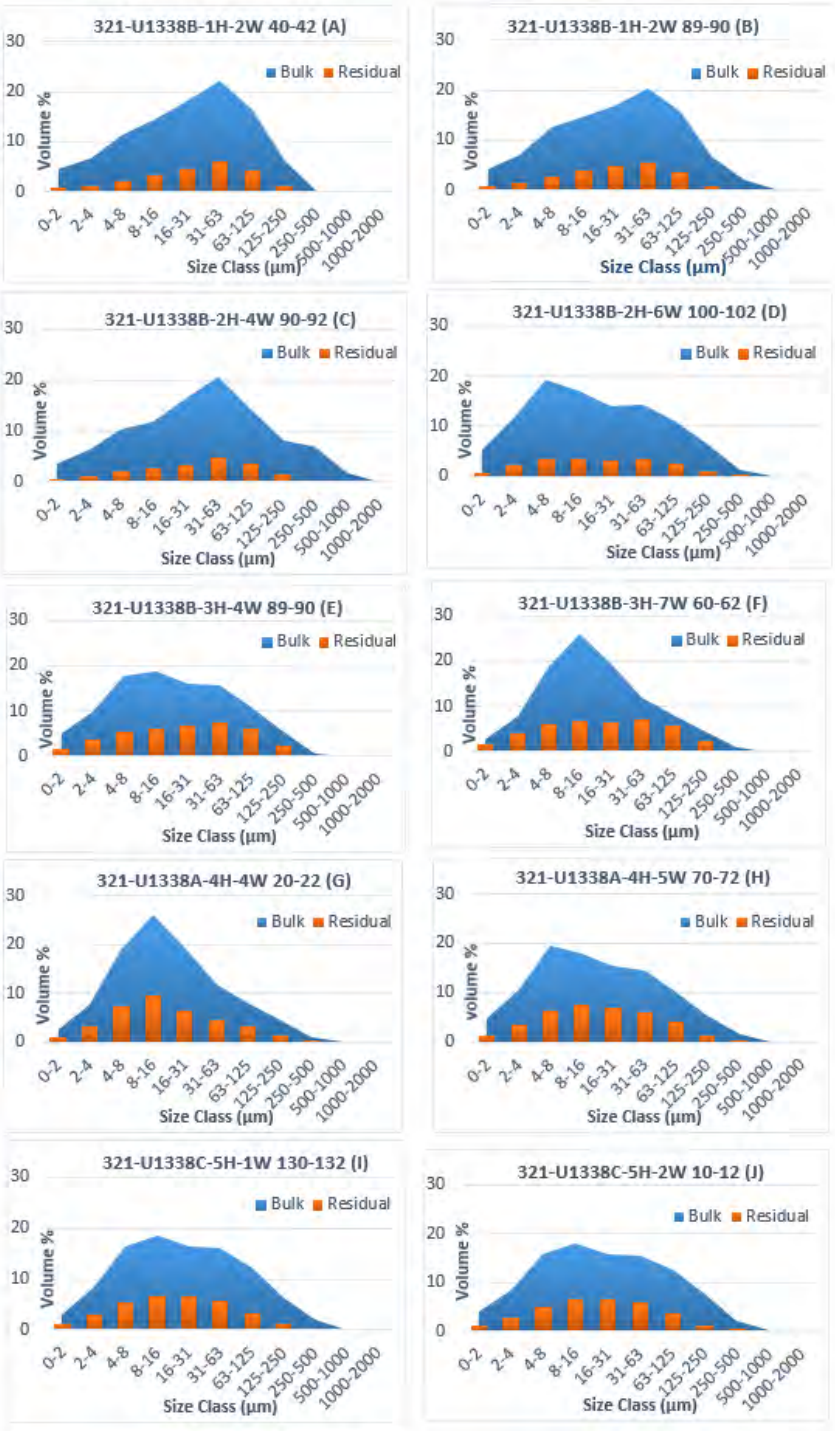

Figures 9A-9J; Grain size distribution profiles for Site U1338 scaled using published measurements of % $CaCO_3$. The blue profile represents bulk sediment. The orange bars show the residual material after removal of carbonate.

Bulk sediment

In Site U1338, the first three and shallowest samples (Fig 9A,9B,9C) show a similar general pattern with peaks in grain size at around 4-8 µm, 31-63 µm and 250-500 µm (Fig 9C). The 4-8 µm (fig 9A-9C) would account for calcareous nannofossils that fall within the range of 1-20 µm (fig 1). The distribution from 2-16 µm is gradually increasing but there is an absence of a distinct and very pronounced peak. This could have to do with the rather moderate and varying preservation (good-poor) in the sedimentary succession from Site U1338. The 31-63 µm would account for planktonic foraminifera and foraminiferal fragments but also some benthic foraminifera. The foraminifera fragments may be the least contributing component because of the good preservation of foraminifera. The peak between 250-500 µm should account for the different foraminifera. However, the mentioned boundaries for the different organisms are approximate and can vary depending on oceanographic setting. Particle sizes exceeding 63 µm would account for big foraminifera.

Figure 9D display peaks at 4-8 µm and 31-63 µm. The same peaks are seen for Figure 9E with an addition of 31-63 µm. This would imply that Figure 9E has a larger contribution of foraminifera in it. Since the planktonic foraminifers differ in a big way from rare to abundant, a more pronounced inclusion of those in 8E is logical.

Figures 9F and 9G show distinct peaks at 8-16 µm relating to coccoliths while an increase in residual components is observed at the coarser end of the profile.

Figures (9H, 9I, 9J) show similar patterns in grain size distribution. Fig 9H peak at 4-8 µm and 31-63 µm and the other two at 4-8 µm 8-16 µm and 31-63µm. A similar distribution of foraminifera and foraminiferal fragments is observed by the more or less even profile shapes.

Residual

In general, the residual material is evenly distributed throughout the profiles (9A-9J). This is supported by the smear slides (Table 7) that include intact and fragmented diatoms and radiolaria throughout the samples which creates a wider range of grain sizes. The residual peaks are often correlated with the peaks of the bulk. At 9E-9J the residual material increases with relation to the decreased carbonate percentage (table 14). A lot of fragmented radiolaria and diatoms are observed (table 7).

Figures 9A-9D show a peak in residual material at 31-63 µm. Thereafter

Site 926

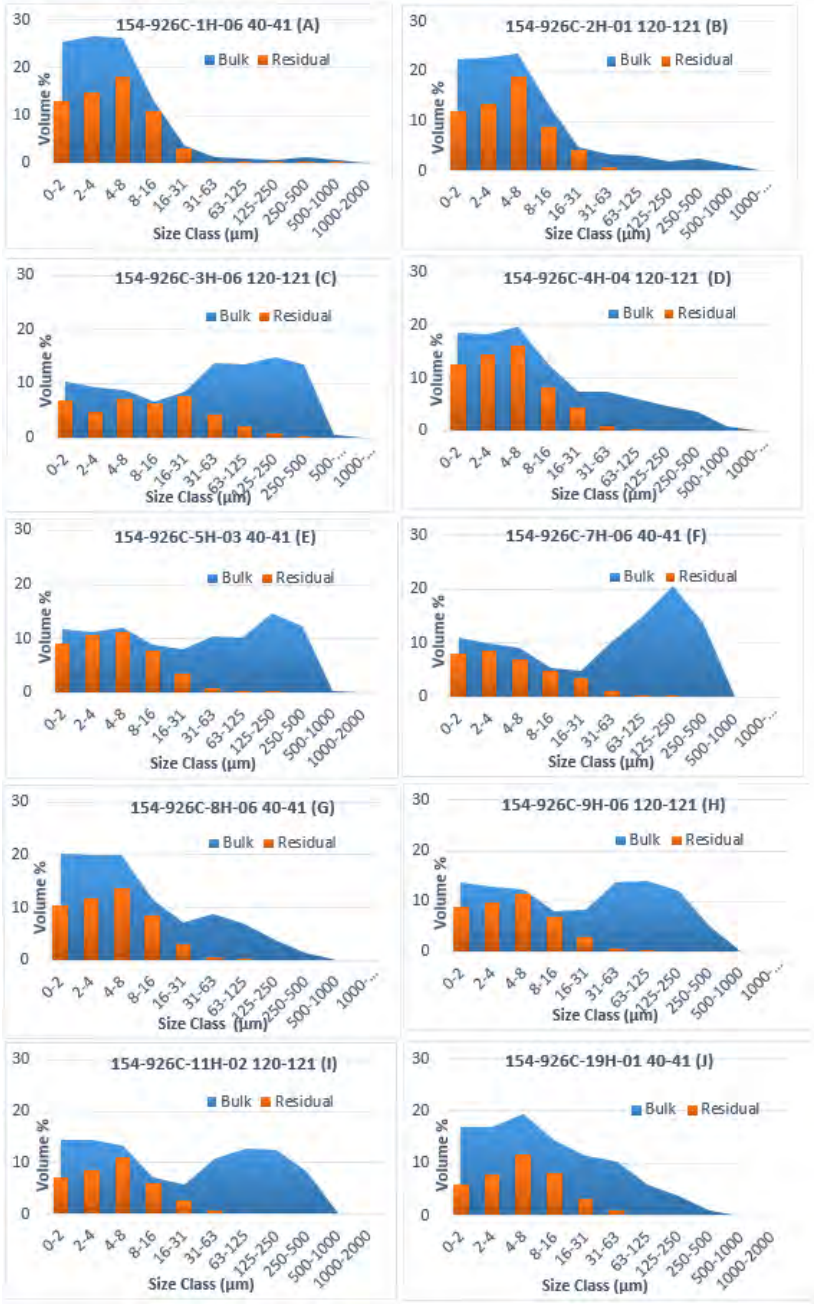

Figures 10A-10J; Grain size distribution profiles for Site 926 scaled using published measurements of % $CaCO_3$. The blue profile represents bulk sediment. The orange bars show the residual material after removal of carbonate.

Bulk Sediment

Figures 10A, 10B, 10D show similar grain size distribution and bulk vs residual volumetric relationships for the Site 926 samples but the form is quite different to Site U1338 (Fig.9). The bulk sediment tends to be concentrated within 2-16 µm implying that the carbonate is largely made up of calcareous nannofossils. Between these samples, Figure 10D has a higher volume from 31 µm and higher grain size, indicating a larger content of foraminifera. Since the preservation in Site 926 is in generally very good, foraminifera fragments would maybe not have a significant contribution to the carbonate content.

Figures 10C, 10E, 10H peak at about 0-2 µm, 4-8 µm, 31-63 µm and 125-250 µm. The majority of the volume percentages are seen going from 31 µm and higher grain size. A significant contribution of foraminifera to the carbonate could be the reason. Figure 10F has a very pronounced peak at 125-250 µm, displaying the highest mode to the carbonate. The carbonate in Figure 10G is mostly made up of nannofossil ooze as indicated by the high volume between 2-16 µm. A small peak is seen at 31-63 µm relating to foraminifera. Figure 10I show modes at 4-8 µm and 31-63 µm while also having a more smooth transition from smaller to larger grain sizes.

Residual

The clay particles have a size range of <4 µm while silt ranges from 4-63 µm and different types of sand from 63 µm-1000 µm. Importantly, as seen on the figures, in all Site 926 samples, the residual material is accounting for a bigger part of the bulk for most of the samples compared to Site U1338. The residual material is mostly seen between 2-63 µm (accounting for clay, silt and very fine sand) but also at 63-125 µm (fine sand). These terrigenous particles were observed in smear slides (table 10).

Site 756

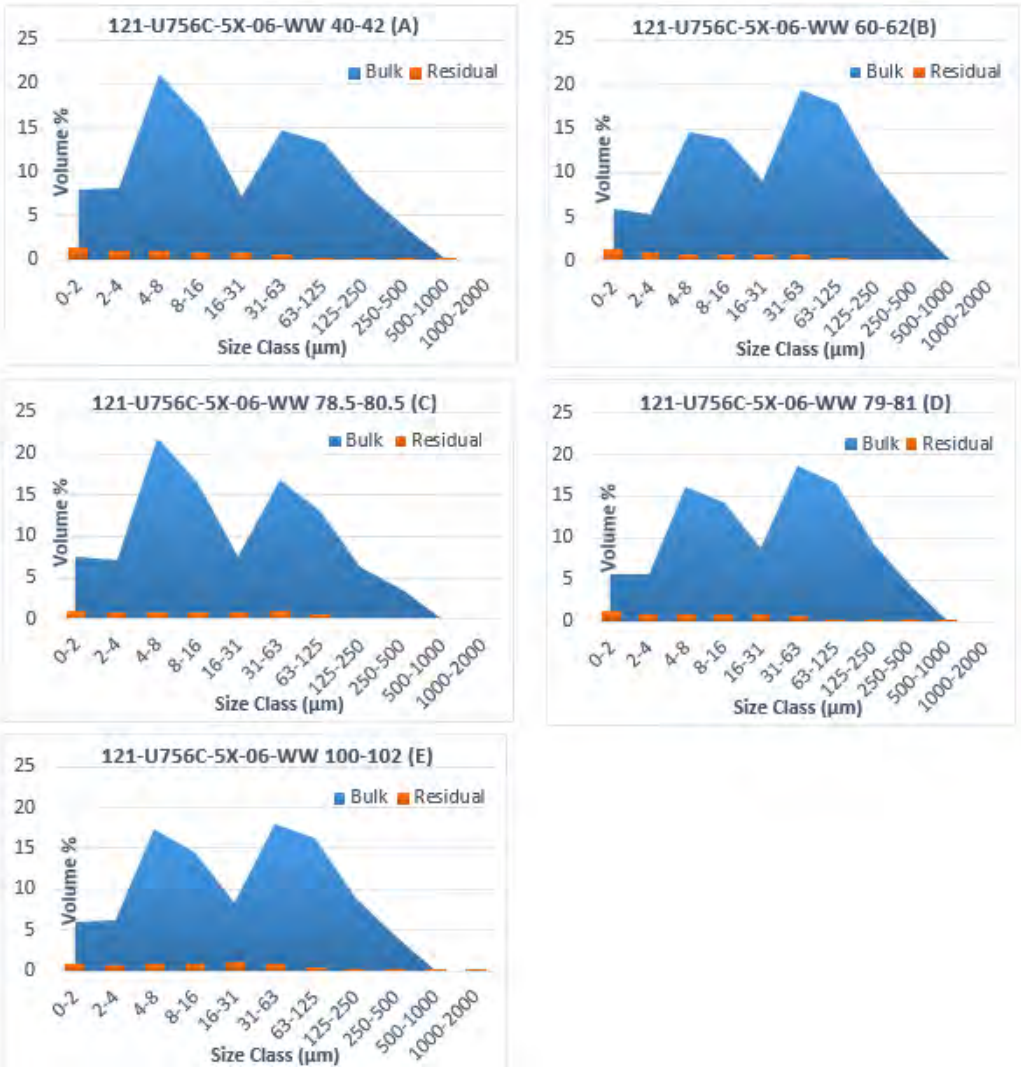

Figure 11A-11E; Grain size distribution profiles for Site 756 scaled using published measurements of % $CaCO_3$. The blue profile represents bulk sediment. The orange bars show the residual material after removal of carbonate.

The bulk compared with residual profiles for Site 756 are different again.

Figures 11A-11E show a similar general profile shape in the bulk sediment grain size distribution spectra and minimal contributions of non-carbonate material. There are two distinct modes in the bulk, which we can consider as dominantly carbonate in this case, between 2-16 µm and 31-125 µm. All of the figures show a dip in volume between 16-31 µm corresponding to smaller amounts of for foraminiferal

fragments. Figures 11A and 11C show the highest peaks between 2-16 µm indicating a considerable coccolith content. The other smaller but distinct peaks between 31-125 µm would account for a larger inclusion of foraminifera. Figures 11B, 11D & 11E are to the majority made up of foraminifera indicated by the highest peak going from 31 µm and beyond. In general this unit (1A) should be dominated by nannofossils with foraminifera (Peirce and Weissel, et al., 1989).

Comparison of sediment grain size distribution between sites

The sediment grain size distribution profiles between the sites are very different. The profiles from Site U1338 (Figures 9A-9J) show a more evenly distributed grain size pattern compared to the other sites. This would have to do with the abundance of the different carbonate and siliceous organisms (that have a wide variance in size range) due to the location of the Site in the EEP characterized by a high primary productivity due to upwelling. Modes are seen at 4-8 µm, 31-63 µm for fig 9A, 9B and 9C (+ 250-500 µm) which indicates a more even contribution of different carbonate components (nannofossils, foraminifera) to the bulk. The top three samples indicate a dominance of foraminifera and there is a shift to coccoliths at depth in the bulk profiles. The residual shows a shift from 31-63 µm to 8-16 µm mode at the bottom. The distribution of carbonate is more even in a general sense, compared to the patterns seen in Figures 10A-10J from Site 926.

The grain size distribution profiles for Site 926 (figures 10A-10J) is differing from Site U1338. Figures 10A-10J show a greatly varying distribution between the samples with depth. The bulk curves show a very contrasting pattern with the majority of the material either concentrated to the left (smaller grain sizes) or to the right (larger grain sizes). Figures 10A, 10B show that the volume is parked within the size ranges of 2-16 µm implying that coccoliths are the dominant carbonate components. A similar pattern is seen for 10D, 10G and 10J with the exception of a higher volume within >63 µm with order, implying a higher fraction of foraminifera. Figure 10C and 10E have pretty even distributions but with slightly higher volumes towards larger grain sizes (>31 µm). Figures 10H and 10I are very coherent showing rather equal distributions to either side of 16-31 µm. Most of the samples show a dip in volume around 16-31 µm which could be related to a scarce distribution of foraminiferal fragments as indicated by the generally very good preservation of carbonate components in Site 926**.** The residual material is making up a big part of the volume as compared to Site U1338 that has lower volumes of residual components (table 14). The bulk sediment from Site 926 was darker in color compared to the sediment from U1338 when seen visually. Most of the residual material is seen between 2-16 µm accounting for clay and silt. Further, Site 926 lies with a proximity to the Amazon River that generates great inputs of terrigenous material into the surrounding area. This is further supported by figures 10A-10J that show high volumes of residual terrigenous material which is especially dominant in the 3 shallowest and youngest samples (Figures 10A, 10B & 10C). These samples from the Pleistocene have the lowest $CaCO_3$ content averaging to 35% between them (table 14). Since the last 16 m.y. sedimentation rates have progressively increased from around 12 cm/k.y. to around 33 cm/k.y. during Pleistocene (Curry and Cullen, 1997). Figure 10C is somewhat of an anomaly, showing residual material after 63 µm. This would be very fine

to fine sand. Figure 10F show a peak at 125-250 µm which could be some big foraminifera. The sediment distribution profiles are very contrasting to those from Site U1338, showing a higher variability in grain size distribution over time.

The grain size distribution profiles for Site 756, figures 11A-11E (the practice samples to develop the procedure) are very different to the other sites. The carbonate components are very dominant, making up most of the bulk as indicated by the average carbonate content of 94% (table 14) and the very low volumes of residual material. Since these samples are from the same core and section not much variability is seen through time.

Comparison of bulk sedimentary data with the theoretical model

The theoretical carbonate profile (figure 1), predicts that the calcaerous nannofossils range between 1-20 µm with a pronounced peak at 5 µm. The calcareous nannofossils that live in the shallow surface mixed layer where the coccoliths thrive due to the excess of nutrients provided by upwelling and a high input of solar radiation which promotes primary production. The foraminiferal fragments range between 30-40 µm with a peak at 38 µm. At 63 µm a third peak is illustrated which accounts for planktic foraminifera and benthic foraminifera that range from 55 µm towards higher grain sizes (fig1). I have not attempted to isolate the $CaCO_3$ particle distribution profiles due to the lack of sample specific weights and $CaCO_3$. However below some thought is given to the general distribution patterns.

Site U1338

If comparing the individual overlayed bulk samples from Site U1338 (fig 6A), peaks are falling within rather similar grain size ranges. Visually they are not alike because of the different scale of the size classes. For the theoretical model (fig 1) there are sharp peaks at 5 µm, 38 µm and 63 µm compared to 5-7 µm, 10-15 µm, and 40-50 µm (fig 6A). There are similarities but there are not sharp and distinctive boundaries for the obtained data set (fig 6A) compared to figure 1. In general the overlayed bulk:residual relationship illustrated by figures 9A-9J often show peaks at 4-8 µm, 8-16 µm and 31-63 µm. The first two (4-8 µm, 8-16 µm) fall within the range of 1-20 µm for calcareous nannofossils (fig 1), and 31-63 µm is another peak that includes a peak between 30-40 µm and another at 63 µm within 55 µm and higher grain sizes) in figure 1.

Site 926

Fig 7A, display comparable peaks to figure 1, at between 3-5 µm and 60 µm which correlate pretty well with the two peaks (5 µm & 63 µm) seen in (figure 1). Figure 7A is also showing peaks at 200 µm and 300 µm which is not comparable with figure 1.

Site 756

Figure 8A, display peaks at 6-8 µm and 50-70 µm which is comparable to two peaks seen in figure 1. 6-8 µm is comparable to the calcareous nannofossils in fig 1, while 50-70 µm is comparable to the one for foraminifera in fig 1. Figures 11A-11E display sharp peaks at 4-8 µm and 31-63 µm that is also comparable.

General

The comparisons mentioned above for all of the sites with respect to figure 1 are possible if seen from a perspective emphasizing on the mode. However, the ratio between calcareous nannofossils, foraminifera fragments etc. for all sites are not directly comparable with the theoretical figure that show more sharp boundaries and a clear boundary of nannofossils to the bulk. Volume percentages are more evenly distributed between the different particles (nannofossils, foraminifera etc.) for the profiles from the three sites compared to figure 1. However, the data sets obtained show some peaks that are comparable while other modes observed in the data set are absent in the theoretical profile (figure 1). Figure 1, show sharp boundaries between the carbonate components (coccoliths, foraminiferal fragments etc) and it is not backed up by observations.

Reproducibility

The method used is not ultimate since the grain size analyzer measures the particles in volume %, assuming a spherical shape for all of the particles. This gives a significant source of error since the grain size distribution profiles obtained will not be entirely accurate. Another issue is beam steering that can be caused by the dispersant that changes the refractive index which can be misleading, measuring coarse particles that are not really there. This could be the case if the sample are being partially dissolved in the dispersant (Malvern Instruments Ltd, 2011). For example, figure 12 is showing a rather poor reproducibility indicated by the 90th percentile Dx90. Figure 13 is indicating a coherent relationship between a sample and its 7 66replicate. The poor reproducibility could be related to a potential dissolution of carbonate particles in the stirring dispersant and further indicated by the decreased laser obscuration signal. The residual

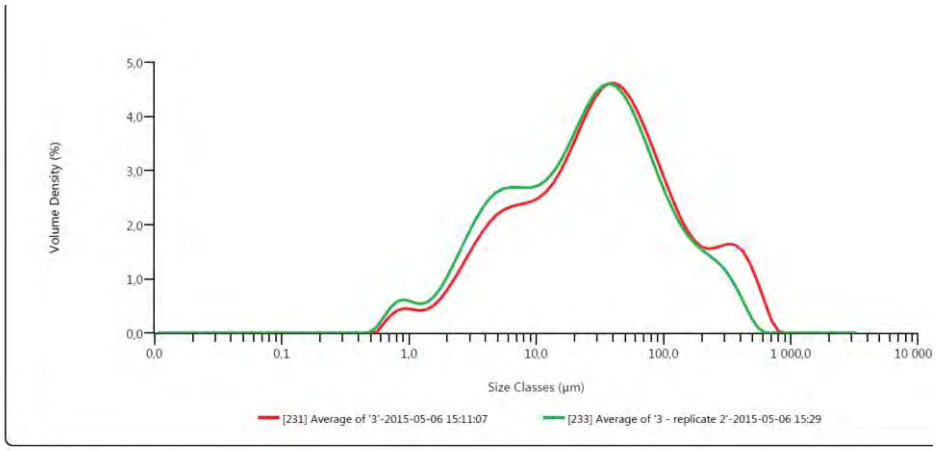

	Record Number	Sample Name	Dx (10) (µm)	Dx (50) (µm)	Dx (90) (µm)	Laser Obscuration (%)
	231	Average of '3'	4,08	33,1	220	8,24
	233	Average of '3 - replicate 2'	3,32	26,6	143	11,40
Mean			**3,70**	**29,9**	**182**	**9,82**
1xStd Dev			**0,535**	**4,57**	**54,6**	**2,23**
1xRSD (%)			**14,5**	**15,3**	**30,1**	**22,76**

Figure 12; Overlayed relationship between Bulk sample 321-U1338B-2H-4W 90-92 (fig 9C) and the replicate of it.

samples and replicates showed a smaller standard deviation between them (fig 14). There seem to be a relationship between the poor reproducibility and the carbonate.

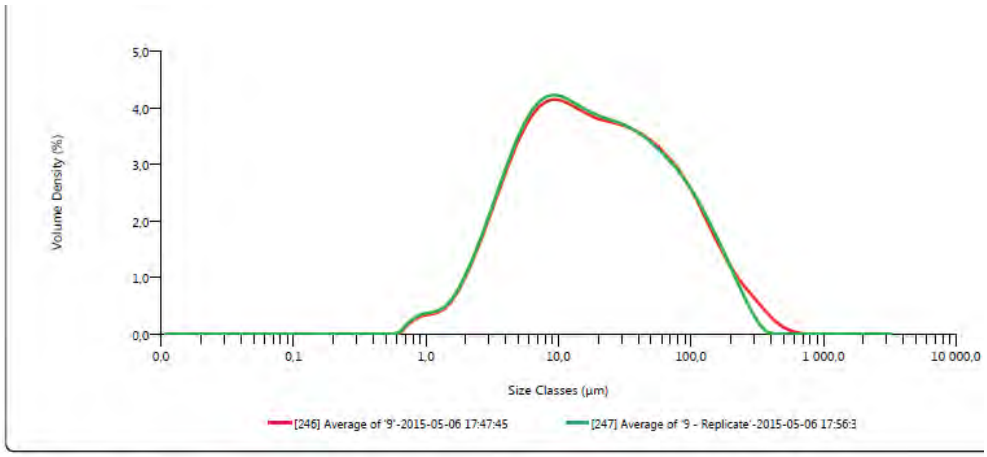

	Record Number	Sample Name	Dx (10) (µm)	Dx (50) (µm)	Dx (90) (µm)	Laser Obscuration (%)
	246	Average of '9'	3,63	18,3	114	3,92
	247	Average of '9 - Replicate'	3,54	17,4	105	7,11
Mean			**3,59**	**17,9**	**110**	**5,51**
1xStd Dev			**0,0610**	**0,615**	**6,16**	**2,26**
1xRSD (%)			**1,70**	**3,44**	**5,62**	**40,97**

Figure 11; Overlayed relationship between bulk sample 321-U1338C-5H-1W 130-132 (fig. 9I) and the replicate.

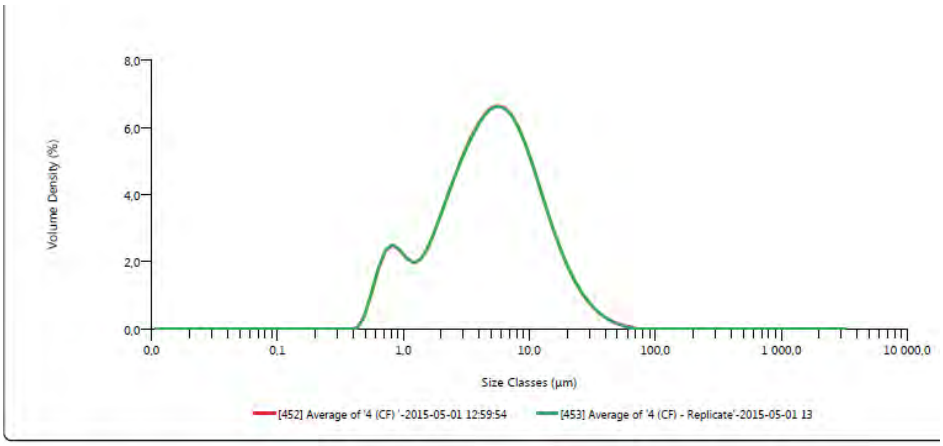

	Record Number	Sample Name	Dx (10) (µm)	Dx (50) (µm)	Dx (90) (µm)	Laser Obscuration (%)
	452	Average of '4 (CF) '	1,09	4,86	14,6	8,67
	453	Average of '4 (CF) - Replicate'	1,08	4,86	14,7	11,29
Mean			**1,08**	**4,86**	**14,6**	**9,98**
1xStd Dev			**0,00706**	**0,00143**	**0,0263**	**1,85**
1xRSD (%)			**0,653**	**0,0294**	**0,180**	**18,52**

Figure 14; Overlayed relationship between residual sample 154-926C-3H-06 120-121 (fig. 10C) and the replicate.

Limitations of the method

The grain size analyzer assumes that all of the particles are spheres in order to perform measurements and calculations to give the particles a quantitative number. This is a potential source of error in generating the grain size profiles since the sediment components are not spherical; especially the biogenic particles that may be discoid, pennate, globular or highly ornate and irregular. Another limitation is that the grain-size analyzer only records/measures the particles within the "area" of the light, so to say the particles that are hit by the laser analyzer under the time of measurement which is 30 seconds. We have minimized this error source by optimizing the settings with enhanced stirring speed. Since the machine makes five measurements per sample, it should give a fair and representative value of the whole sample. Another factor to take into consideration is that big particles can ruin the reliability of the data by taking up a big part of the volume. Therefore it is important to homogenize the effectively. The bulk samples were homogenized using a spatula. There is also a risk of putting too much force on the samples when homogenizing, which can break up some carbonate particles. This can result in less accurate distribution profiles. The multiple acidifications, especially for the samples from Site 926 could have also effected size and shape of the residual particles due to chemical dissolution.

The Acidification of Ceara Rise Samples: All of the samples went through the same amount of acidic washes (15) but samples 6-10 reacted more vigorously, and for longer (created more fizzing and bubbles) compared other samples, when reaching the latter stages of the acidification process. This could indicate that the carbonate content is increasing with depth for these samples and this is something that is consistent with % $CaCO_3$ measurements from the IODP report which shows a general trend of increasing carbonate with depth.

Limitation of the acetic acid treatment: Since it was hard to dissolve the carbonate with buffered acetic acid, large volumes (43.5 liters) was required to account for the 27 washes for all the sites together. This was time-consuming and expensive. The question of whether a stronger acid e.g. hydrochloric would dissolve the carbonate particles much faster, arose. It was concluded, however, that this approach could be more damaging to the residual particles (e.g. clays, silicates), thus introducing a new source of error. Buffered acetic acid is what is normally used for dissolving carbonate. Following this discussion, to aid the digestion process, for samples from site U1338, more effort was put into homogenizing the samples in a mortar pestle. This resulted in 6 acidic washes to get rid of the carbonate, compared to 15 washes for Site 926 from the Ceara Rise that also has less carbonate than Site U1338 from the equatorial Pacific where there is more primary productivity. Another possibility in the future may be to increase the reaction rate by heating the samples beforehand. This was not attempted in this study in order to keep a consistent procedure of all of the sites.

A significant limitation of this study is the fact that the dry weight of the bulk sediment and de-carbonated residual was not measured. While this would be straightforward to obtain the bulk dry weight in the future it would take more time to recover, dry and weigh the residual. Here I dealt with the lack of this data by using published measurements of carbonate content % from the respective IODP/ODP references from each site and in that way reducing the residue values to modify the profiles

making them more presentable and easier to discuss. A limitation here is that the % $CaCO_3$ values (table 14) used were only averages for nearby samples. However, this approach allows a realistic estimate of the ratio between carbonate: non-carbonate in the bulk sediment to be calculated.

An alternative for the future would be to try putting bulk sample into the grain size analyzer, perform the measurement and then add hydrochloric acid directly to the reaction vessel of the instrument to dissolve the carbonate in-situ. The resulting grain size distribution profile of the residual would also reflect the actual residual volume compared to the bulk because the grain size density had genuinely decreased as a result of the digestion of carbonate. Since the Hydro LV (the reaction vessel/volume-unit that controls the wet dispersion of the particles) of the grain size analyzer is made of Teflon stainless steel it is not affected by the acid. This was not clear to me at the onset of the study. One concern is that the acid and the reaction products would maybe change the absorption- and refraction index of the dispersant when measuring the residual material. This would maybe have some influence, since the background was measured in deionized water before injecting the sample. This effect however would likely be small and the advantages would still overweigh the disadvantages.

Conclusion

The first attempt at producing diagnostic profiles that show variability with time and between different ocean settings was productive in a sense. The method was effective at removing carbonate and the separate bulk and residual profiles show clear differences in grain size distribution patterns that are consistent with the mineral content and differing a lot from each other due to their specific oceanic setting. Grain size distribution curves were obtained showing the relationship between bulk and residual. The dominant grain size-classes are within 2-16 µm and 31-63 µm, implying a great contribution of nannofossil to the bulk. A lot of questions and issues have arisen in connection with the method used in this project. There has not been success in extracting carbonate grain size profiles due to the lack of $CaCO_3$ % for the samples. However, indications from the bulk and residual profiles suggest that they do not look similar to the model (fig 1), which predicts more distinctive boundaries between particles size classes. However, there are elements of the distribution pattern that do match carbonate grain size peaks in the theoretical profile. Limitations of the method effect the accuracy of the results and these have to be thought of for future experiments with the method used. This may not be an optimal method and it has to be evaluated further in order to provide qualitative and accurate data for measuring bulk stable isotopes.

Acknowledgements

First of all I would like to thank my supervisors Eve Arnold and Helen Coxall for their guidance, advice and encouragements. I would also want to thank Jan Backman for helping me with the smear slides. My thanks go to Carina Johansson and Therese Granberg for their support. I would like to thank the Integrated Ocean Drilling Program (IODP) and Ocean Drilling Program (ODP) for providing the samples. Very special thanks goes to my parents, Amel and Bouraoui, my brothers Elias and Slim for always being there and supporting me through life. I also want to thank Foad who I consider a brother and all my friends and family in France, Sweden and Tunisia.

References

Articles

Buhrke, V. E., Jenkins, R., & Smith, D. K. (1998). *A practical guide for the preparation of specimens for x-ray fluorescence and x-ray diffraction analysis*. New York: Wiley-VCH.

Curry, W.B., Shackleton, N.J., and Richter, C., et al. 1995a, Introduction: Proceedings of the Ocean Drilling Program, Initial Reports, Leg 154: *College Station, Texas, Ocean Drilling Program*) v. 154 p.5-10.

Curry, W.B., Cullen, J.L., 1997. Carbonate production and dissolution in the western equatorial Atlantic during the last 1 M.y.. Proc. ODP Sci. Results 154, p.189 - 199.

Curry, W.B., Shackleton, N.J., and Richter, C., et al. 1995b: Proceedings of the Ocean Drilling Program, Initial Reports, Leg 154, Site 926: *College Station, Texas, Ocean Drilling Program*) v.154 p.153-232.

Frenz, M., K.-H. Baumann, B. Boeckel, R. Hoppner, and R. Henrich (2005), Quantification of foraminifer and coccolith carbonate in South Atlantic surface sediments by means of carbonate grain-size distributions, *J. Sediment. Res.*, 75,464–475.

Gibbs, S. J., N. J. Shackleton, and J. R. Young (2004), Identification of dissolution patterns in nannofossil assemblages: A high-resolution comparison of synchronous records from Ceara Rise, ODP Leg 154, *Paleoceanography*, 19, doi:10.1029/2003PA000958

Heather M. Stoll, Daniel P. Schrag, Coccolith Sr/Ca as a new indicator of coccolithophorid calcification and growth rate, *Geochemistry, Geophysics, Geosystems*, 2000, 1, 5, n/a

Heinrich S, and K.A.F. Zonneveld., 2013, Influence of the Amazon River development and constriction of the Central American Seaway on Middle/Late Miocene oceanic conditions at the Ceara Rise: Palaeogeography. Palaeoclimatology. Palaeoecology., 386 (2013), pp. 599–606

Joseph J. Lalicata, David W. Lea, Pleistocene carbonate dissolution fluctuations in the eastern equatorial Pacific on glacial timescales: Evidence from ODP Hole 1241, *Marine Micropaleontology*, 2011, **79**, 1-2, 41

Krause, J.W., Nelson, D.M., Brzezinski, M.A., 2011. Biogenic silica production and the diatom contribution to primary production and nitrate uptake in the eastern equatorial Pacific Ocean. Deep-Sea Research II 58 (3–4), 434–448

Kumar, N, Embley, R (1977) Evolution and origin of the Ceara rise: An aseismic rise in the western equatorial Atlantic. Bull. Geol. Soc. Am. 88: pp. 683-694

LaMontagne, R. W., R. W. Murray, K.-Y. Wei, M. Leinen, and C.-H. Wang (1996), Decoupling of carbonate preservation, carbonate concentration, and biogenic accumulation: A 400-kyr record from the central equatorial Pacific Ocean, *Paleoceanography*, ,553–562.

Lawrence, K.T., Liu, Z., Herbert, T.D., 2006. Evolution of the eastern tropical Pacific through Plio-Pleistocene glaciation. Science 312, 79-83.

Lawrence, K. T., Zhonghui, L. & Herbert, T. D. Evolution of the eastern tropical Pacific through Plio-Pleistocene glaciation. Science 312, 79–83 (2006)

Lyle, M, Pälike, H, Nishi, H, Raff, I, Gamage, K, Klaus, A (2010) The Pacific Equatorial Age Transect, IODP Expeditions 320 and 321: building a 50-million-year-long environmental record of the equatorial Pacific Ocean. Sci Drill 9: pp. 4-15

Malvern Instruments Ltd, 2011, *Mastersizer 3000 User manual*, MANO474 Issue 1.0, 2011, Worcestershire, United Kingdom

Peirce, J., Weissel, J., et al., 1989. Leg 121 background and objectives. *Proceedings of the Ocean Drilling Program, Initial Reports.,* 121: College Station, Texas (Ocean Drilling Program), p.5-31
Pennington, J.T., Mahoney, K.L., Kuwahara, V.S., Kolber, D.D., Calienes, R., Chavez, F.P., 2006. Primary production in the eastern tropical Pacific: a review. Progress in Oceanography 69 (2–4), 285–317.

Pälike, H., Lyle, M., Nishi, H., Raffi, I., Gamage, K., Klaus, A., 2010 and the Expedition 320/321 Scientists, *Proc. IODP,* 320/321: Tokyo (Integrated Ocean Drilling Program Management International, Inc.), Site U1338, doi:10.2204/iodp.proc.320321.110.2010

Reghellin., D., Coxall H.K., Dickens G.R., Backman J., carbon and oxygen isotopes of bulk carbonate in sediment deposited beneath the Eastern Equatorial Pacific over the last 8 million years. *Department of Geological Sciences, Stockholm University, SE-106 91 Stockholm*, Sweden. P.1-33.

Books

Sam Boggs Jr, 2011*, Principles of Sedimentology and Stratigraphy,* fifth edition, Pearson Education Inc, New Jersey, USA